

Manifestation of a strong electroweak sector with decoupling at hadronic colliders

R. Casalbuoni and D. Dominici

Dipart. di Fisica, Univ. di Firenze, Largo E. Fermi, 2, I-50125 Firenze

and I.N.F.N., Sezione di Firenze, Largo E. Fermi, 2, I-50125 Firenze

P. Chiappetta and A. Deandrea

Centre de Physique Théorique, CNRS Luminy, Case 907, F-13288 Marseille Cedex 9*

S. De Curtis

I.N.F.N., Sezione di Firenze, Largo E. Fermi, 2, I-50125 Firenze

R. Gatto

Département de Physique Théorique, Univ. de Genève, 24 quai E.-Ansermet, CH-1211 Genève 4

(February 1997)

Abstract

We study the expected phenomenology at present (Tevatron) and future (Tevatron Upgrade, LHC) hadronic colliders of a model describing a strong electroweak symmetry breaking sector with both vector and axial vector strong interacting bosons degenerate in mass. Due to decoupling, this model at low energies is almost indistinguishable from the Standard Model, passing therefore all low energy precision tests at LEPI. We will show that it gives

*Unité Propre de Recherche 7061

quite visible signals at forthcoming hadronic accelerators. The new charged vector bosons can be detected more easily than the neutral ones.

I. INTRODUCTION

Future hadron colliders offer the possibility of testing the electroweak symmetry breaking sector by studying WW scattering. It is well known that if no new physics, like supersymmetry, enters to guarantee a low mass Higgs, some new strong interaction must become manifest at a scale of the order of 1 TeV. The standard technicolor [1] or the walking technicolor [2] are particular models of a dynamical breaking of the electroweak symmetry. Their rich phenomenology at hadron colliders has been recently reexamined [3]. One can also perform a model independent analysis of a strong interacting electroweak sector, by studying chiral effective lagrangians. Usually one takes into account the following three possible scenarios. In the first no resonance in the WW channel is formed and one has just the sector of the longitudinal gauge bosons strongly interacting [4]. In the second scenario the WW interactions give rise to a scalar resonance (Higgs remnant) [5]. In the third scenario the resonance is formed in the $J = I = 1$ channel, and a new triplet of gauge vector bosons is present [6]. The phenomenology at hadron colliders of these three different scenarios has been largely studied [7] and it has been recently reviewed in ref. [8].

LEPI results have drastically constrained the strong mechanism for electroweak symmetry breaking, namely rescaled QCD technicolor scenarios are ruled out. In this paper we will focus on a scheme of dynamical symmetry breaking in which decoupling is automatically satisfied in the low energy limit, therefore the deviations from the Standard Model (SM) are strongly suppressed. This model, called degenerate BESS (BESS standing for Breaking Electroweak Symmetry Strongly), has been proposed in a previous work [9], to which we refer the reader for details.

In brief the spirit of the model is the following. We start from the global symmetry group of the theory $G = SU(2)_L \otimes SU(2)_R$, spontaneously broken to the diagonal subgroup $H_D = SU(2)_V$. The new vector and axial vector bosons correspond to the gauge bosons associated to a hidden symmetry, $H' = SU(2)_L \otimes SU(2)_R$. The symmetry group of the theory becomes $G' = G \otimes H'$. It breaks down spontaneously to H_D and gives rise to nine

Goldstones. Six of these are absorbed by the vector and axial vector bosons. As soon as we perform the gauging of the subgroup $SU(2)_L \otimes U(1)_Y \subset G$, the three remaining Goldstones disappear giving masses to the SM gauge bosons. This general procedure for building models with vector and axial vector resonances is discussed in [10].

What makes the model [9] so attractive is the fact that all the deviations in the low energy parameters from their SM values are strongly suppressed. This allows the existence of a strong electroweak sector at relatively low energies within the precision of electroweak tests, such that it may be accessible with accelerators designed for the near future. As such it offers possibilities of experimental tests even with future or existing machines of relatively low energy. The phenomenological implications will be discussed below.

The study of the virtual effects of the heavy resonances has previously been done, so we shall now concentrate on their direct production at hadronic colliders. The Tevatron limits on W' are used to constrain the parameter space of degenerate BESS. A feature of degenerate BESS, as compared to BESS with only vector resonances, is the absence of direct coupling of the new resonances to the longitudinal weak gauge bosons. This implies larger widths into fermion pairs as compared to widths into pairs of weak gauge bosons.

Our phenomenological applications include discussion of the properties of the heavy resonances (masses, partial widths) and studies of their effects at the Tevatron upgrade and at the LHC, including rough detector simulation.

In section 2 we recall briefly the main features of the model and give the relevant formulas for the evaluation of the heavy resonances direct production. Subsequently we study the phenomenology related to their discovery at hadron colliders.

II. THE DEGENERATE BESS MODEL

The model includes two new triplets of vector bosons (L^\pm, L_3, R^\pm, R_3). The parameters of the model are a new gauge coupling constant g'' and a mass parameter M , related to the scale of the underlying symmetry breaking sector. We therefore parameterize the model in

terms of g'' and M . In the following we give approximate formulas in the limit $M \rightarrow \infty$ and $g'' \rightarrow \infty$ [11]. For the numerical analysis the exact formulae of [9] were used.

In the charged sector the fields R^\pm are unmixed for any value of g'' . Their mass is given by:

$$M_{R^\pm}^2 \equiv M^2 \quad (1)$$

The charged fields W^\pm and L^\pm have the following masses:

$$\begin{aligned} M_{W^\pm}^2 &= \frac{v^2}{4} g^2, \\ M_{L^\pm}^2 &= M^2(1 + 2x^2) \end{aligned} \quad (2)$$

where $x = g/g''$, g is the usual $SU(2)$ gauge coupling constant and $v^2 = 1/(\sqrt{2}G_F)$.

In the neutral sector we have:

$$\begin{aligned} M_Z^2 &= \frac{M_W^2}{c_\theta^2} \\ M_{L_3}^2 &= M^2(1 + 2x^2) \\ M_{R_3}^2 &= M^2(1 + 2x^2 \tan^2 \theta) \end{aligned} \quad (3)$$

where $\tan \theta = s_\theta/c_\theta = g'/g$ and g' is the usual $U(1)_Y$ gauge coupling constant. Notice that for small x all the new vector resonances are degenerate in mass.

The charged part of the fermionic lagrangian is

$$\mathcal{L}_{charged} = - \left(a_W W_\mu^- + a_L L_\mu^- \right) J_L^{(+)\mu} + H.c. \quad (4)$$

where

$$\begin{aligned} a_W &= \frac{g}{\sqrt{2}} \\ a_L &= -gx \end{aligned} \quad (5)$$

apart from higher order terms and $J_L^{(+)\mu} = \bar{\psi}_L \gamma^\mu \tau^+ \psi_L$ with τ^+ the combination $(\tau_1 + i\tau_2)/2$.

Let us notice that the R^\pm are not coupled to the fermions.

For the neutral part we get

$$\begin{aligned}
\mathcal{L}_{neutral} = & -\left\{ e J_{em}^\mu \gamma_\mu + \left[A J_L^{(3)\mu} + B J_{em}^\mu \right] Z_\mu \right. \\
& + \left[C J_L^{(3)\mu} + D J_{em}^\mu \right] L_{3\mu} \\
& \left. + \left[E J_L^{(3)\mu} + F J_{em}^\mu \right] R_{3\mu} \right\}
\end{aligned} \tag{6}$$

where γ_μ in the preceeding formula is the photon field and again in the limit $M \rightarrow \infty$, $x \rightarrow 0$,

$$\begin{aligned}
A &= \frac{g}{c_\theta} & B &= -\frac{g s_\theta^2}{c_\theta} \\
C &= -\sqrt{2} g x & D &= 0 \\
E &= \sqrt{2} g \frac{x}{c_\theta} \tan^2 \theta & F &= -E
\end{aligned} \tag{7}$$

and $J_{em}^\mu = Q \bar{\psi} \gamma^\mu \psi$, $J_L^{(3)\mu} = \bar{\psi}_L \gamma^\mu T_L^3 \psi_L$ are the usual neutral currents.

The total fermionic widths are

$$\begin{aligned}
\Gamma_{L_3}^{fermion} &= \frac{2\sqrt{2} G_F M_W^2}{\pi} M_{L_3} \left(\frac{g}{g''} \right)^2 \\
\Gamma_{R_3}^{fermion} &= \frac{10\sqrt{2} G_F M_W^2}{3\pi} \frac{s_\theta^4}{c_\theta^4} M_{R_3} \left(\frac{g}{g''} \right)^2 \\
\Gamma_{L^\pm}^{fermion} &= \frac{2\sqrt{2} G_F M_W^2}{\pi} M_{L^\pm} \left(\frac{g}{g''} \right)^2
\end{aligned} \tag{8}$$

while from the trilinear gauge couplings we get the following widths:

$$\begin{aligned}
\Gamma_{L_3}^{WW} &= \frac{\sqrt{2} G_F M_W^2}{24\pi} M_{L_3} \left(\frac{g}{g''} \right)^2 \\
\Gamma_{R_3}^{WW} &= \frac{\sqrt{2} G_F M_W^2}{24\pi} \frac{s_\theta^4}{c_\theta^4} M_{R_3} \left(\frac{g}{g''} \right)^2 \\
\Gamma_{L^\pm}^{WZ} &= \frac{\sqrt{2} G_F M_W^2}{24\pi} M_{L^\pm} \left(\frac{g}{g''} \right)^2
\end{aligned} \tag{9}$$

It may be useful to compare the widths of the new gauge bosons into vector boson pairs with those into fermions:

$$\begin{aligned}
\Gamma_{L_3}^{fermion} &= 48 \Gamma_{L_3}^{WW} \\
\Gamma_{R_3}^{fermion} &= 80 \Gamma_{R_3}^{WW} \\
\Gamma_{L^\pm}^{fermion} &= 48 \Gamma_{L^\pm}^{WZ}
\end{aligned} \tag{10}$$

We see that the total fermionic channel is dominant due to the multiplicity.

III. DEGENERATE BESS AT TEVATRON

Data from the Fermilab Tevatron Collider, collected by the CDF collaboration [12] put limits on the model parameter space. Their search was done through the decay $W' \rightarrow e\nu_e$, assuming standard couplings of the W' to the fermions. Their result can be translated into a limit for the degenerate BESS model parameter space.

In Fig. 1 these limits are shown in terms of the mass of the R^\pm resonance, M , and the ratio of coupling constants, $x = g/g''$. The present limit from CDF obtained with an integrated luminosity of 19.7 pb^{-1} (dashed line) is compared with the result obtained from LEPI (continuous line). Limits from LEPI are obtained calculating virtual effects up to order M_W^2/M^2 , and using the experimental data from ref. [13]. Note that in the low energy limit ($M \rightarrow \infty$) there are no deviations from the SM, thus allowing to consider light new resonances for the strong sector. The figure was obtained using the CDF 95% C.L. limit on the W' cross-section times the branching ratio and comparing this limit with the predictions of our model at fixed g/g'' , thus giving a limit for the R^\pm mass. This procedure was then iterated for various values of g/g'' . The statistical significance of the plot is that of a 95% C.L. limit in one variable, the mass, at a given value of g/g'' . The CDF limit is presently less restrictive than the LEPI one. While waiting for the analysis of 100 pb^{-1} , we have considered an extrapolation of the CDF data based on the principle that when the background is present the cross-section limit scales inversely with the square root of the luminosity [14]. The extrapolation of the CDF bound to an integrated luminosity of 100 pb^{-1} (dotted line) improves marginally LEPI result and only for masses of the new vector resonances smaller than 400 GeV.

We will now study the detection of charged and neutral vector resonances from a strong electroweak sector at the upgrading of the Fermilab Tevatron [14]. The option we have chosen is the so called TeV-33, with a c.m. energy of the collider of 2 TeV and an integrated luminosity of 10 fb^{-1} . We have considered the total cross-section $p\bar{p} \rightarrow L^\pm, W^\pm \rightarrow \mu\nu_\mu$ and compared it with the SM background. A minimum of 10 events per year has been required

to detect the signal with respect to the background. If no deviations are seen within the statistical error and a systematic error of 5% on the cross-section, we get the 90% C.L. bound shown in Fig. 2.

Up to a region of 1 TeV the limits from TeV-33 option are stronger with respect to LEPI (we recall that LEPII will only marginally improve LEPI results [9]).

The events were simulated using Pythia Montecarlo [15]. The simulation was performed using the expected detector resolution, in particular a smearing of the energy of the leptons was done according to $\Delta E/\sqrt{E} = 10\%$ and the error in the 3-momentum determination was assumed to be between 3% for a mass of the order of 500 GeV and 5% for a mass of 1000 GeV.

We have first analyzed the production of the charged resonances L^\pm of the degenerate BESS in the channel $p\bar{p} \rightarrow \mu\nu_\mu$. Only Drell-Yan mechanism for production was considered since it is the dominant one (see the couplings and widths listed in the previous section). The signal events were compared with the background from SM muon-neutrino production. Two cases have been analyzed, namely a mass of 400 GeV for the new charged resonances with $g/g'' = 0.12$ (Fig. 3) and $M = 600$ GeV with $g/g'' = 0.2$ (Fig. 4). The first case is taken in a region of the parameter space, which is allowed at present, but is expected to be soon excluded at Tevatron when all data will be analyzed (100 pb^{-1}). The second choice of the parameters of the model is instead testable only with the TeV-33 option. The observable we deal with is the transverse mass of the charged resonance.

We now consider the production of the neutral resonances of the model, and their subsequent decay into muon pairs. This is the cleanest signature, but the production rate is less favourable than for the new charged bosons. As a consequence the best exclusion limits that can be imposed on the parameter space originate from non-observation of charged resonances. In order to compare the neutral boson production to the charged one, we have taken in Figs. 5 and 6, the same values for the parameters as in Figs. 3 and 4. The observable in this case is the invariant mass of the muon pair.

We have examined various cases with different choices of M , and g/g'' (taken inside the

physical region shown in Fig. 1) to give an estimate of the sensitivity of the model to this option for the upgrading of the Tevatron (see Tables 1 and 2). For each case we have selected cuts to maximize the statistical significance of the signal. We see that the number of signal events decreases for increasing mass of the resonance. The conclusion is that Tevatron with the high luminosity option will be able to discover a strong electroweak resonant sector as described by the degenerate BESS model for masses up to 1 TeV. It can be seen from the calculation of the statistical significance (see Tables 1 and 2) that the charged process allows to push further the discovery limits of the new vector bosons at Tevatron with respect to the neutral process. However the experimental check of the model requires the proof of the existence of both neutral and charged vector bosons. Notice that the reconstruction of the resonance mass requires a careful study of the experimental setup, due to the smallness of the resonance width.

IV. DEGENERATE BESS AT THE LHC

The physics of the Large Hadron Collider (LHC) has been discussed in a number of papers (see [16] and references therein); it will be able either to discover the new resonances or to constrain the physical region left unconstrained by previous data. We have considered a configuration of LHC with a c.m. energy $\sqrt{s} = 14$ TeV, a luminosity of $10^{34} \text{ cm}^{-2} \text{ s}^{-1}$ and one year run (10^7 s).

If no new resonances are discovered, limits can be imposed on the parameter space of the model. We have considered the total cross-section of $pp \rightarrow L^\pm, W^\pm \rightarrow \mu\nu_\mu$, which has a clear signature and a large number of events, and we have compared it with the SM background of $\mu\nu_\mu$. We have obtained a contour plot at 90% C.L. in the two variables M and g/g'' , shown in Fig. 7.

The applied cuts were $|p_{t\mu}| > M/2 - 50 \text{ GeV}$ in order to maximize the deviation of BESS model cross-section with respect to the SM one (most of the SM events are low p_t ones). Moreover we have assumed a systematic error of 5% in the cross-section and the

statistical error obtained considering a luminosity of $10^{34} \text{cm}^{-2} \text{s}^{-1}$ (dotted-dashed line) or of $10^{33} \text{cm}^{-2} \text{s}^{-1}$ (dotted line) and one year run (10^7 s). The new resonances of the model can be discovered directly for a wide range of values of the parameter space of the model. The discovery limit in the mass of the resonance depends on the value of g/g'' . For example if $g/g'' = 0.1$, the resonance is visible over the background at least up to 2 TeV.

In Figs. 8-12 we show the differential distribution of events at LHC of $pp \rightarrow L^\pm, W^\pm \rightarrow \mu\nu_\mu$ in the transverse mass of the new vector boson for different values of M and g/g'' . The choice we have done is within the region not accessible to the upgrading of the Tevatron. The energy of the muons was smeared by 10% and the error in the 3-momentum increases with the momentum of the muon from 3% to 9% as stated in [17].

In particular in Fig. 8 a light resonance mass $M = 500 \text{ GeV}$ and $g/g'' = 0.15$ is considered. Once cuts have been applied the number of signal events per year is approximately 85000 whereas the corresponding background consists of 26000 events. The smearing of the muon momentum is taken equal to 3% in this case.

In Fig. 9 only g/g'' is changed, in order to illustrate the LHC sensitivity to the BESS parameters. When g'' gets larger the number of events decreases as $1/g''^2$.

In Figs. 10-12 we show cases corresponding respectively to $M = 1, 1.5, 2 \text{ TeV}$ with $g/g'' = 0.1$. The smearing of the muon momentum is taken equal to 5, 7, 9% respectively.

The statistical significance of the previous examples is given in Table 3, showing that the discovery of a charged resonance up to 2 TeV with $g/g'' \simeq 0.1$ is well within the reach of LHC. The limit of detection for a 2 TeV mass is reached for a value of $g/g'' = 0.03$.

We will finally consider the production and decay of the corresponding neutral resonances of the model in Figs. 13-17, using the same values for the BESS parameters as in the charged channel examined before.

Although the number of events is smaller, neutral vector bosons up to 2 TeV, provided g/g'' is not smaller than 0.1, can be seen (see Table 4).

V. CONCLUSIONS

We have discussed an effective theory describing new vector and axial vector resonances within the scheme of a strong electroweak breaking sector.

The new vector and axial vector particles are degenerate in mass (at the leading order) and their virtual effects are suppressed, allowing the model to pass all low energy precision tests at LEPI. In the low energy limit ($M \rightarrow \infty$ with the gauge coupling of the new resonances fixed) the new particles are decoupled and we obtain the effective lagrangian of the SM. High energy hadron colliders, as Tevatron and LHC, will allow to study the direct production of new resonances from Drell-Yan mechanism. With actual Tevatron luminosity, it is not possible to improve LEPI bounds on degenerate BESS parameter space. This is no more the case when the upgrade in luminosity of Tevatron is considered. If the new particles are not discovered at LHC, stringent bounds on the model parameters are derived.

The direct observation of the new resonances is possible in a wide range of the parameter space of the model, up to the 1 TeV range at Tevatron and up to 2 TeV at LHC, in some case with a spectacular number of events.

Acknowledgements

This work has been carried out within the Program Human Capital and Mobility: “Tests of electroweak symmetry breaking and future European colliders”, CHRXCT94/0579, BBW/OFES 95.0200. A.D. acknowledges the support of a TMR research fellowship of the European Commission under contract nr. ERB4001GT955869. We thank D.Fouchez for discussion on PYTHIA Montecarlo at an early stage of this work.

REFERENCES

- [1] S.Weinberg, Phys. Rev. **D19**, 1277 (1979); L.Susskind, Phys. Rev. **D20**, 2619 (1979).
- [2] B.Holdom, Phys. Rev. **D24**, 1441 (1981), Phys. Lett. **B150**, 301 (1985); T.Appelquist, D.Karabali and L.C.R.Wijewardhana, Phys. Rev. Lett. **57**, 957 (1986); T.Appelquist and L.C.R.Wijewardhana, Phys. Rev. **D36**, 568 (1987); K.Yamawaki, M.Bando and K.Matsumoto, Phys. Rev. Lett. **56**, 1335 (1986); T.Akiba and T.Yanagida, Phys. Lett. **B169**, 432 (1986).
- [3] E.Eichten and K.Lane, FERMILAB-CONF-96/297-T, BUHEP-96-33, hep-ph/9609297, FERMILAB-CONF-96/298-T, BUHEP-96-34, hep-ph/9609298.
- [4] T.Appelquist and C.Bernard, Phys. Rev. **D22**, 200 (1980); A.C.Longhitano, Phys. Rev. **D22**, 1166 (1980), Nucl. Phys. **B188**, 118 (1981).
- [5] M.B.Einhorn, Nucl. Phys. **B246**, 75 (1984); R.Casalbuoni, D.Dominici and R.Gatto, Phys. Lett. **B147**, 460 (1984).
- [6] R.Casalbuoni, S.De Curtis, D.Dominici and R.Gatto Phys. Lett. **B155**, 95 (1985), Nucl. Phys. **B282**, 235 (1987).
- [7] M.S.Chanowitz, M.K.Gaillard, Phys. Lett. **B142**, 85 (1984); Nucl. Phys. **B261**, 379 (1985); R.S.Chivukula, Proceedings of the 12th Johns Hopkins Workshop, Baltimore 1988, eds. G.Domokos and S.Kövesi-Domokos; R.Casalbuoni, P.Chiappetta, S.De Curtis, F.Feruglio, R.Gatto, B.Mele and J.Terron, Phys. Lett. **B249**, 130 (1990); A.Dobado, M.J.Herrero and J.Terron, Z. Phys. **C50**, 205 (1991); *ibidem* 465 (1991); J.Barger, S.Dawson and G.Valencia, Nucl. Phys. **B399**, 364 (1993); J Bagger, V.Barger, K.Cheung, J.Gunion, T.Han, G.A.Ladinsky, R.Rosenfeld, C.P.Yuan, Phys. Rev. **D49**, 1246 (1994), hep-ph/9504426; S. De Curtis, hep-ph/9610356.
- [8] M.Golden, T.Han and G.Valencia, UCD-95-32, hep-ph/9511206.

- [9] R.Casalbuoni, A.Deandrea, S.De Curtis, D.Dominici, R.Gatto and M.Grazzini, Phys. Rev. **D53**, 5201 (1996), hep-ph/9510431.
- [10] R.Casalbuoni, S.De Curtis, D.Dominici, F.Feruglio and R.Gatto, Int. Jour. Mod. Phys. **A4**, 1065 (1989).
- [11] R.Casalbuoni, S.De Curtis, D.Dominici and M.Grazzini, Phys. Lett. **B388**, 112 (1996), hep-ph/9607276.
- [12] F.Abe et al., Phys. Rev. Lett. **74**, 2900 (1995).
- [13] G.Altarelli, CERN-TH/96-265, hep-ph/9611239.
- [14] Report of the TeV-2000 Study Group, Editors D.Amidei and R.Brock, FERMILAB-PUB-96/082, April 1996.
- [15] T.Sjostrand, Comp. Phys. Comm. **82**, 74 (1994).
- [16] *Large Hadron Collider Workshop*, Proceedings of the Workshop, edited by G.Jarlskog and D.Rein, CERN 90-10, ECFA 90-133, 1990.
- [17] ATLAS letter of intent, CERN/LHCC/92-4, LHCC/I2 (1992).

TABLES

g/g''	M	Γ_{L^\pm}	$ p_t^\mu _c$	m_T	$\#B$	$\#S$	$S/\sqrt{S+B}$
	GeV	GeV	GeV	GeV			
0.12	400	0.4	150	300	385	887	24.9
0.20	600	1.7	200	400	82	303	15.4
0.40	1000	11.1	300	800	0	16	4.0

TABLE I. Degenerate BESS at Tevatron Upgrade for the process $p\bar{p} \rightarrow L^\pm \rightarrow \mu\nu_\mu + X$. For all the cases we have also applied a cut $|p_t^{miss}|_c = |p_t^\mu|_c$. Here $\#B(S)$ corresponds to the number of background (signal) events.

g/g''	M	Γ_{L_3}	Γ_{R_3}	$ p_t^\mu _c$	$m_{\mu^+\mu^-}$	$\#B$	$\#S$	$S/\sqrt{S+B}$
	GeV	GeV	GeV	GeV	GeV			
0.12	400	0.4	0.06	150	300	269	257	11.2
0.20	600	1.7	0.03	200	500	33	106	9.0
0.40	1000	11.1	1.64	300	800	1	3	1.5

TABLE II. Degenerate BESS at Tevatron Upgrade for the process $p\bar{p} \rightarrow L_3, R_3 \rightarrow \mu^+\mu^- + X$. Here $\#B(S)$ corresponds to the number of background (signal) events.

g/g''	M	Γ_{L^\pm}	$ p_t^\mu _c$	m_T	$\#B$	$\#S$	$S/\sqrt{S+B}$
	GeV	GeV	GeV	GeV			
0.075	500	0.2	150	400	26300	20780	95.8
0.15	500	0.8	150	400	85477	26300	255.0
0.1	1000	0.7	300	800	2050	3130	43.5
0.1	1500	1.0	500	1300	247	469	17.5
0.1	2000	1.4	700	1800	41	118	9.4

TABLE III. Degenerate BESS at LHC for the process $pp \rightarrow L^\pm \rightarrow \mu\nu_\mu + X$. For all the cases we have applied a cut $|p_t^{miss}|_c = |p_t^\mu|_c$. Here $\#B(S)$ corresponds to the number of background (signal) events.

g/g''	M	Γ_{L_3}	Γ_{R_3}	$ p_t^\mu _c$	$m_{\mu^+\mu^-}$	$\#B$	$\#S$	$S/\sqrt{S+B}$
	GeV	GeV	GeV	GeV	GeV			
0.075	500	0.2	0.03	150	400	16781	4300	29.6
0.15	500	0.8	0.11	150	400	17480	16781	94.4
0.10	1000	0.7	0.10	300	800	1145	605	14.5
0.10	1500	1.0	0.15	500	1300	146	153	8.8
0.10	2000	1.4	0.20	700	1800	35	22	2.9

TABLE IV. Degenerate BESS at LHC for the process $pp \rightarrow L_3, R_3 \rightarrow \mu^+\mu^- + X$. Here $\#B(S)$ corresponds to the number of background (signal) events.

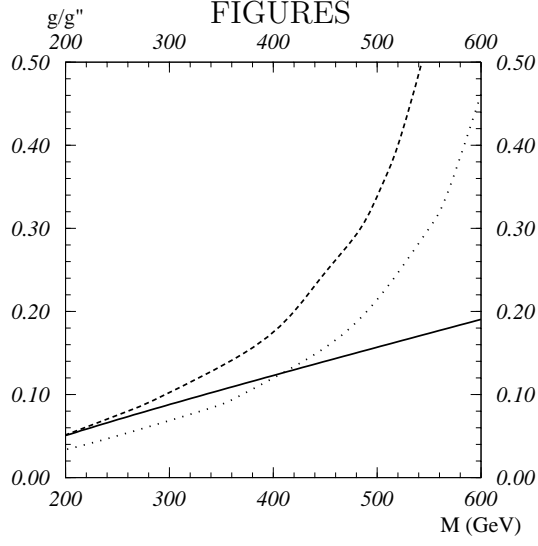


Fig. 1 - 95% C.L. upper bounds on g/g'' vs. M from LEPI data (solid line) and CDF with $L = 19.7 \text{ pb}^{-1}$ (dashed line). The dotted line shows the extrapolation of the CDF bounds to $L = 100 \text{ pb}^{-1}$.

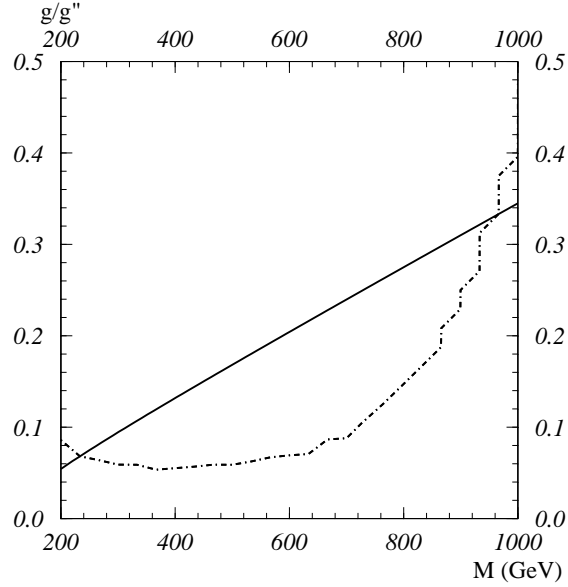


Fig. 2 - 90% C.L. limits on the parameter space $(M, g/g'')$ of degenerate BESS model at Tevatron upgrade with $\sqrt{s} = 2$ TeV and a luminosity of $10^{33} \text{cm}^{-2} \text{s}^{-1}$, supposing no deviation is seen with respect to the SM in the total cross-section $p\bar{p} \rightarrow \mu\nu_\mu$. A minimum of 10 events per year is required to detect the signal with respect to the background; both the statistical error and a systematic error of 5% on the cross-section are taken into account. The applied cuts are $|p_{T\mu}| > M/2 - 50$ GeV. The figure is obtained from a grid of 25x25 cross-section points in the parameter space of the model. The continuous line corresponds to the LEPI limits.

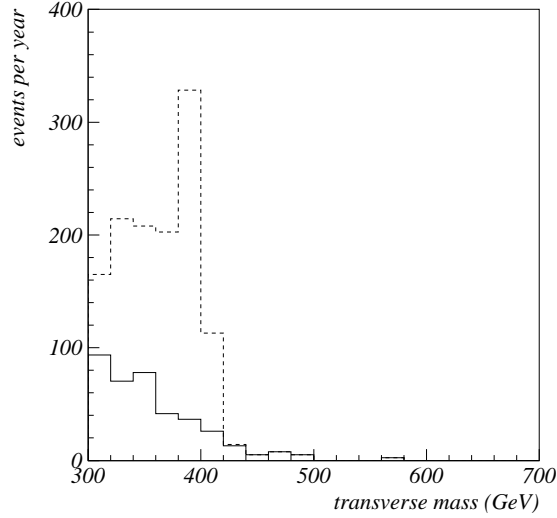


Fig. 3 - Transverse mass differential distribution of $p\bar{p} \rightarrow L^\pm, W^\pm \rightarrow \mu\nu_\mu$ events at Tevatron upgrade with a luminosity of $10^{33} \text{cm}^{-2} \text{s}^{-1}$ and $\sqrt{s} = 2$ TeV, for $M = 400$ GeV, $g/g'' = 0.12$. The following cuts have been applied: $|p_{T\mu}| > 150$ GeV, $m_T > 300$ GeV. The continuous line is the SM background, the dashed line represents the degenerate BESS model signal plus background. The number of signal events per year is 887, the corresponding background consists of 385 events.

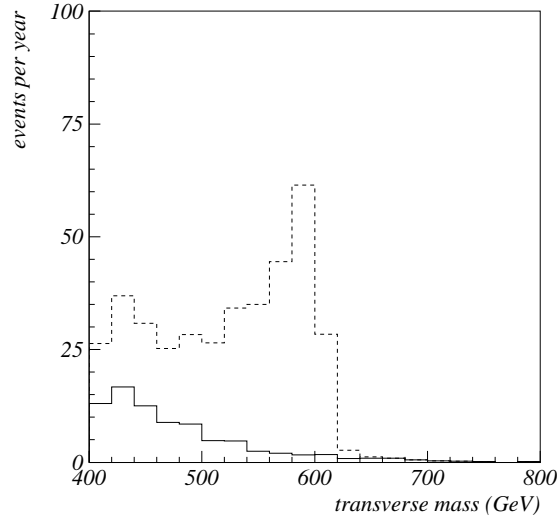


Fig. 4 - Same as in Fig. 3, for $M = 600$ GeV, $g/g'' = 0.2$. The following cuts have been applied: $|p_{T\mu}| > 200$ GeV, $m_T > 400$ GeV. The number of signal events per year is 303, the corresponding background consists of 82 events.

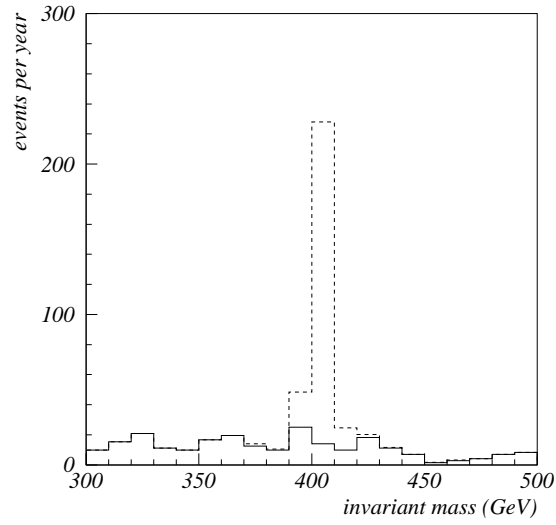


Fig. 5 - Invariant mass differential distribution of $p\bar{p} \rightarrow L_3, R_3, Z, \gamma \rightarrow \mu^+\mu^-$ events at Tevatron upgrade with a luminosity of $10^{33} \text{cm}^{-2}\text{s}^{-1}$ and $\sqrt{s} = 2$ TeV, for $M = 400$ GeV, $g/g'' = 0.12$. The following cuts have been applied: $|p_{T\mu}| > 150$ GeV, $m_{\mu^+\mu^-} > 300$ GeV. The continuous line is the SM background, the dashed line represents the degenerate BESS model signal plus background. The number of signal events per year is 257, the corresponding background consists of 269 events.

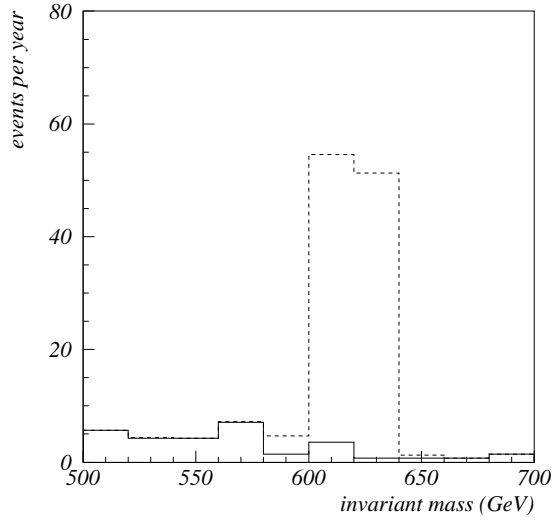


Fig. 6 - Same as in Fig. 5, for $M = 600$ GeV, $g/g'' = 0.2$. The following cuts have been applied: $|p_{T\mu}| > 200$ GeV, $m_{\mu^+\mu^-} > 500$ GeV. The number of signal events per year is 106, the corresponding background consists of 33 events.

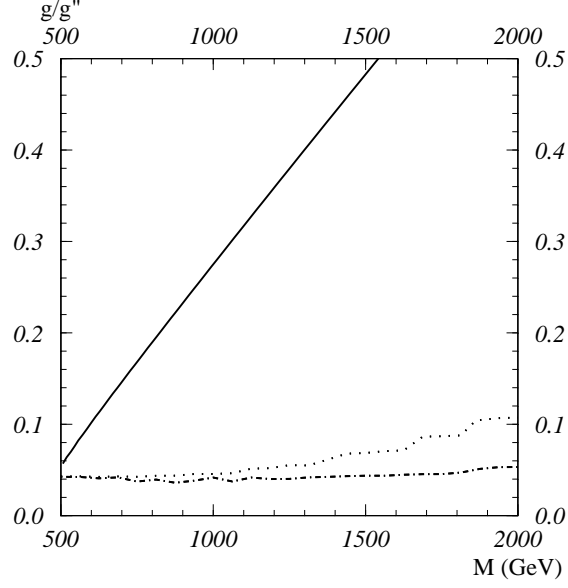


Fig. 7 - 90% C.L. limits on the parameter space $(M, g/g'')$ of degenerate BESS model at LHC with $\sqrt{s} = 14$ TeV and a luminosity of $10^{34} \text{cm}^{-2} \text{s}^{-1}$ (dotted-dashed line) or $10^{33} \text{cm}^{-2} \text{s}^{-1}$ (dotted line), supposing no deviation is seen with respect to the SM in the total cross-section $pp \rightarrow \mu\nu_\mu$. A minimum of 10 events per year is required to detect the signal with respect to the background; both the statistical error and a systematic error of 5% on the cross-section are taken into account. The applied cuts are $|p_{T\mu}| > M/2 - 50$ GeV. The figure is obtained from a grid of 25x25 cross-section points in the parameter space of the model. The continuous line corresponds to LEP limits.

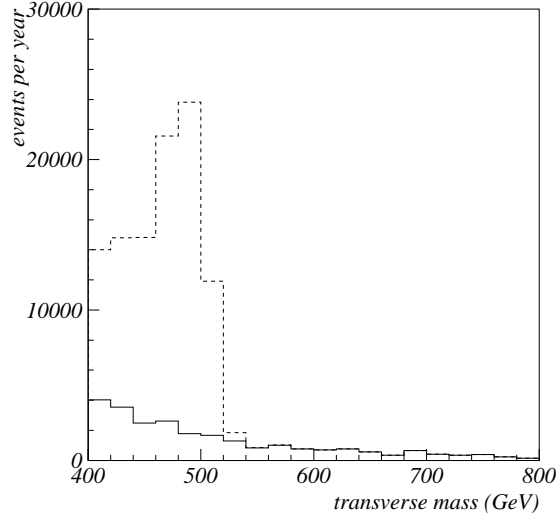


Fig. 8 - Transverse mass differential distribution of $pp \rightarrow L^\pm, W^\pm \rightarrow \mu\nu_\mu$ events at LHC with a luminosity of $10^{34} \text{cm}^{-2} \text{s}^{-1}$ and $\sqrt{s} = 14$ TeV, for $M = 500$ GeV, $g/g'' = 0.15$. The following cuts have been applied: $|p_{T\mu}| > 150$ GeV, $m_T > 400$ GeV. The continuous line is the SM background, the dashed line represents the degenerate BESS model signal plus background. The number of signal events per year is 85477, the corresponding background consists of 26300 events.

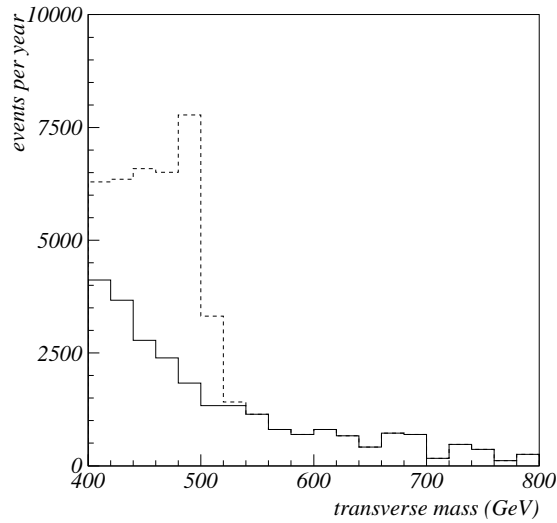


Fig. 9 - Same as in Fig. 8, for $M = 500$ GeV, $g/g'' = 0.075$. The following cuts have been applied: $|p_{T\mu}| > 150$ GeV, $m_T > 400$ GeV. The number of signal events per year is 20780, the corresponding background consists of 26300 events.

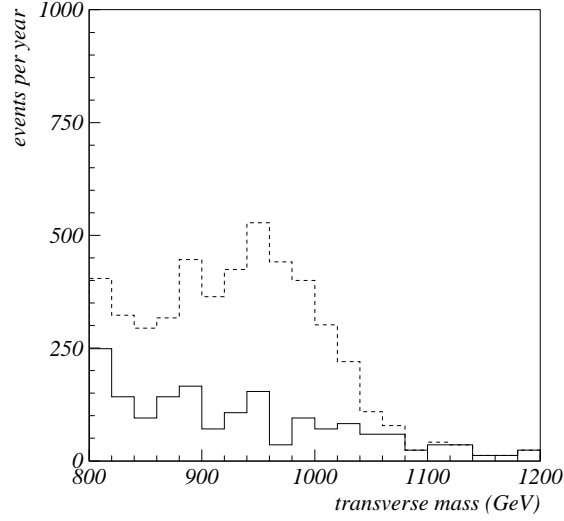


Fig. 10 - Same as in Fig. 8, for $M = 1000$ GeV, $g/g'' = 0.1$. The following cuts have been applied: $|p_{T\mu}| > 300$ GeV, $m_T > 800$ GeV. The number of signal events per year is 3130, the corresponding background consists of 2050 events.

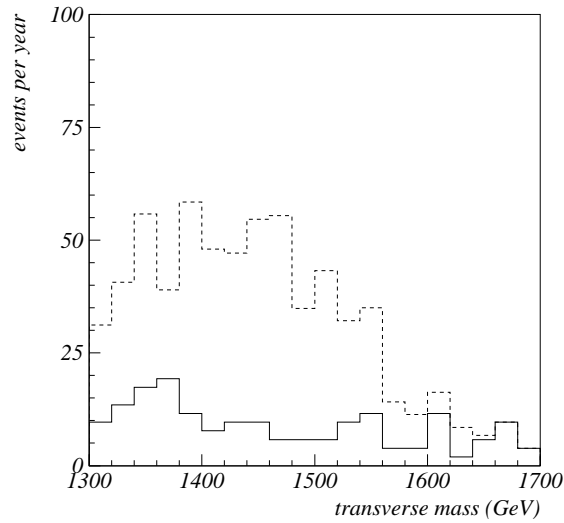


Fig. 11 - Same as in Fig. 8, for $M = 1500$ GeV, $g/g'' = 0.1$. The following cuts have been applied: $|p_{T\mu}| > 500$ GeV, $m_T > 1300$ GeV. The number of signal events per year is 469, the corresponding background consists of 247 events.

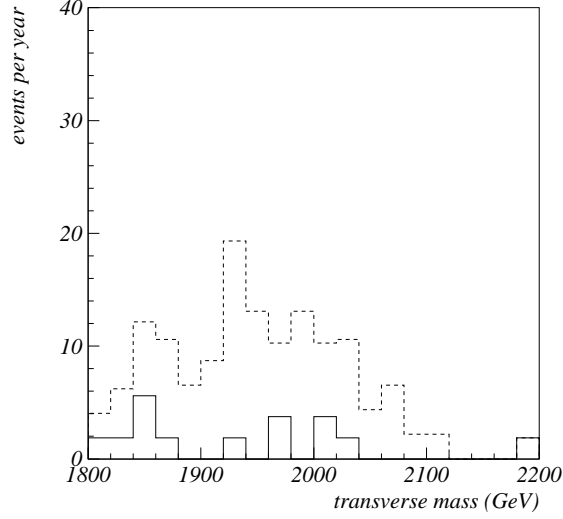


Fig. 12 - Same as in Fig. 8, for $M = 2000$ GeV, $g/g'' = 0.1$. The following cuts have been applied: $|p_{T\mu}| > 700$ GeV, $m_T > 1800$ GeV. The number of signal events per year is 118, the corresponding background consists of 41 events.

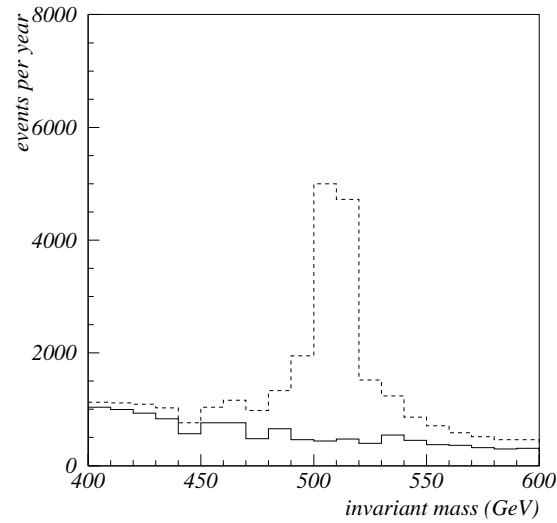


Fig. 13 - Invariant mass differential distribution of $pp \rightarrow L_3, R_3, Z, \gamma \rightarrow \mu^+\mu^-$ events at LHC with a luminosity of $10^{34} \text{cm}^{-2} \text{s}^{-1}$ and $\sqrt{s} = 14$ TeV, for $M = 500$ GeV, $g/g'' = 0.15$. The following cuts have been applied: $|p_{T\mu}| > 150$ GeV, $m_{\mu^+\mu^-} > 400$ GeV. The continuous line is the SM background, the dashed line represents the degenerate BESS model signal plus background. The number of signal events per year is 17480, the corresponding background consists of 16781 events.

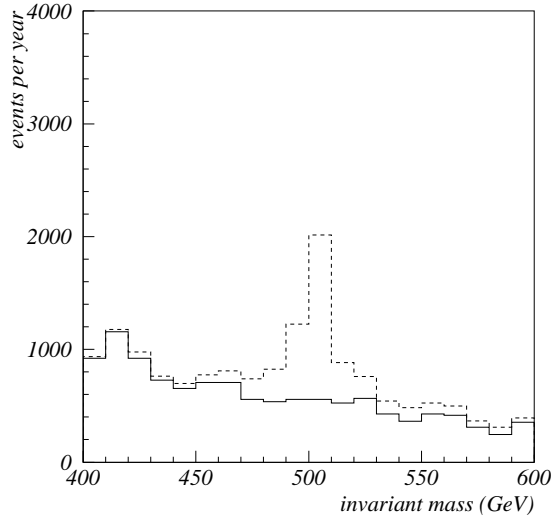


Fig. 14 - Same as in Fig. 13, for $M = 500$ GeV, $g/g'' = 0.075$. The following cuts have been applied: $|p_{T\mu}| > 150$ GeV, $m_{\mu^+\mu^-} > 400$ GeV. The number of signal events per year is 4300, the corresponding background consists of 16781 events.

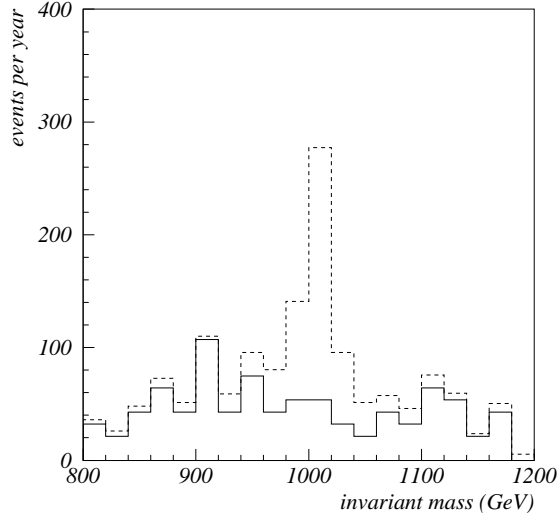


Fig. 15 - Same as in Fig. 13, for $M = 1000$ GeV, $g/g'' = 0.1$. The following cuts have been applied: $|p_{T\mu}| > 300$ GeV, $m_{\mu^+\mu^-} > 800$ GeV. The number of signal events per year is 605, the corresponding background consists of 1145 events.

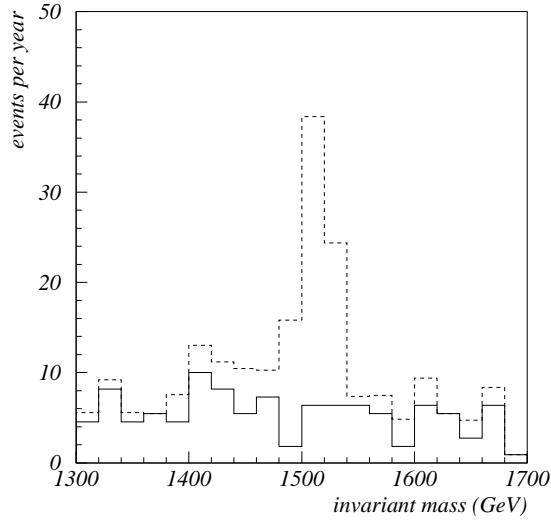


Fig. 16 - Same as in Fig. 13, for $M = 1500$ GeV, $g/g'' = 0.1$. The following cuts have been applied: $|p_{T\mu}| > 500$ GeV, $m_{\mu^+\mu^-} > 1300$ GeV. The number of signal events per year is 153, the corresponding background consists of 146 events.

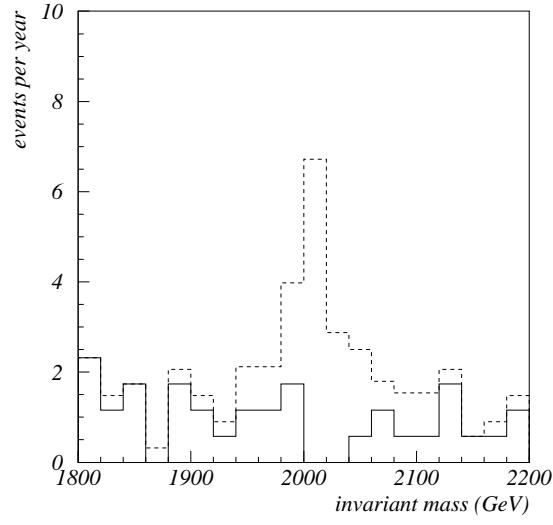


Fig. 17 - Same as in Fig. 13, for $M = 2000$ GeV, $g/g'' = 0.1$. The following cuts have been applied: $|p_{T\mu}| > 700$ GeV, $m_{\mu^+\mu^-} > 1800$ GeV. The number of signal events per year is 22, the corresponding background consists of 35 events.